Proceedings of the XVI National Conference on Superconductivity and Strongly Correlated Systems, Zakopane 2013

Growth and Characterization of $YBa_2Cu_3O_{7-\delta}$ Films Deposited by Laser Ablation on CeO_2-Buffered Sapphire

I. Abal'osheva[a], I. Zaytseva[a], M. Aleszkiewicz[a], A. Malinowski[a], V. Bezusyy[a], Y. Syryanyy[a], P. Gierłowski[a], O. Abal'oshev[a], M. Kończykowski[b] and M.Z. Cieplak[a]

[a]Institute of Physics, Polish Academy of Sciences, al. Lotników 32/46, 02-668 Warszawa, Poland

[b]Laboratoire des Solides Irradies CEA/DSM/IRAMIS &CNRS UMR7642, Ecole Polytechnique, 91128 Palaiseau, France

In this work we study the growth, by pulsed laser deposition, of $YBa_2Cu_3O_{7-\delta}$ (YBCO) films on the CeO_2-buffered R-cut sapphire substrates, with the buffer layer recrystallized prior to the deposition of superconductor. We find that the superconducting critical temperature and the critical current density of the films are very close to similar parameters for the YBCO films grown on lattice-matched single crystalline substrates. It appears that the structural defects in the buffer layer affect the microstructure of YBCO films, resulting in high values of the critical current density, suitable for applications.

DOI: 10.12693/APhysPolA.126.A-69

PACS: 74.78.–w, 77.55.Px, 81.15.Fg

1. Introduction

High-temperature superconducting films, such as thin-film YBCO, find their application in the superconducting microwave filters for the wireless industry due to their very low surface resistance in comparison to the best conducting normal metals [1, 2]. In addition, thin-film YBCO is a perspective material for fault current limiters, provided it displays high critical current density j_c. CeO_2-buffered sapphire is one of the best suited substrates for the growth of thin YBCO films, because of its high thermal conductivity and low cost [3]. However, the thermal expansion coefficient of sapphire is about twice smaller than that of $YBa_2Cu_3O_{7-\delta}$ [4], which frequently results in cracking of the film during cooling down after the deposition. Careful optimization of the thickness of CeO_2 buffer layer is required to avoid the cracking. Recently, we have successfully optimized the growth parameters for a good-quality buffer layer [5]. We have determined that the best procedure involves recrystallization of 30 nm thin CeO_2 buffer layer at a temperature of 1000 °C.

In the present work we examine the growth of YBCO films deposited onto recrystallized CeO_2 buffer layer, in order to maximize the superconducting critical temperature T_{c0} and the j_c. We find good reproducibility of the growth process, with good values of the T_{c0} and j_c in about 70% of the deposited films. We discuss the possible origins of strong vortex pinning in these films.

2. Film preparation and measurement details

The 30 nm thick buffer layers of CeO_2 are grown by pulsed laser deposition (PLD) from ceramic target onto R-cut $(0\bar{2}11)$ Al_2O_3 substrates, which are annealed at 1000 °C prior to deposition. The PLD is performed using Nd:YAG laser (Quanta-Ray Pro 350-10, Spectra Physics) with 4th harmonic generation (laser wavelength 266 nm). The following deposition conditions are found to produce good quality films: pulse duration 9 ns, repetition rate 2 Hz, the energy density on the target 1.5 J/cm^2, substrate temperature 785 °C, and the oxygen pressure in the chamber 400 mTorr. After cooling down to room temperature with the rate of 20 K/min and at the oxygen pressure of 300 Torr, the CeO_2 films are recrystallized inside a tube furnace at 1000 °C in oxygen flow for one hour. Subsequently, the YBCO films, 150 nm thick, are grown on CeO_2 buffer layers, using the same PLD parameters as for the growth of CeO_2 films.

In addition, we also deposit YBCO films on SAT-CAT-La $[(SrAl_{0.5}Ta_{0.5}O_3)_{0.7}(CaAl_{0.5}Ta_{0.5}O_3)_{0.1}(LaAlO_3)_{0.2}]$ substrates, using exactly the same PLD parameters. These substrates have in-plane lattice parameters well-matched to lattice parameters of YBCO, and have been shown to produce films of exceptionally good quality [6]. Here we use these films as a reference, to compare them to films grown on CeO_2-buffered sapphire.

The structural properties of the films are studied using Philips XPert Pro Alpha-1 MPD diffractometer and the surface microstructure is investigated by atomic force microscope (AFM) MultiMode Nanoscope IIIA (Digital Instruments). The samples for four-probe transport DC measurements are patterned by photolithography into 30 and 50 μm wide strips. Transport measurements are performed in the temperature range 4.2 to 300 K. The T_{c0} is determined at $R/R_N = 0.1$, where R is the film resistance and R_N is the normal-state resistance just above the onset of the superconducting transition. The j_c is defined by the criterion of voltage exceeding about 1 μV over 2 mm distance between the voltage leads.

Two non-contact methods, which detect local magnetic induction, are used for additional evaluation of the j_c. The $j_c(T)$-dependence in the T-range down to 4 K is obtained using magnetooptical setup for a Faraday effect

measurement in the iron-garnet indicator, which is placed directly on the top of a superconducting film and inside a magnet. The magneooptical image produced by the magnetic flux penetrating the film is subsequently used to calculate j_c by solving the inverse Biot–Savart problem [7]. The dependence of j_c on the film orientation with respect to the external magnetic field ($H = 2.5$ kOe) is measured in the T-range from 4 to 80 K, using the Hall sensor situated in the film center. The sensor, of the area 20×20 μm^2, is 2-dimensional electron gas device fabricated in a pseudomorphic AlGaAs/InGaAs/GaAs heterostructure. The local magnetic induction measured by a sensor is than used to estimate the j_c [8, 9].

3. Experimental results and discussion

In order to evaluate the reproducibility of the growth process we have carefully measured structural and microstructural properties for a set of 10 films, deposited consecutively, using exactly identical deposition conditions. All films show X-ray diffraction patterns of good-quality YBCO, with c-axis perpendicular to the substrate plane, and negligibly small volume fraction of misaligned grains. However, the films differ slightly by the value of the c-axis lattice parameter. This is depicted in Fig. 1, where the value of c, determined from the (007) X-ray diffraction peak, is plotted against the film number in the film set.

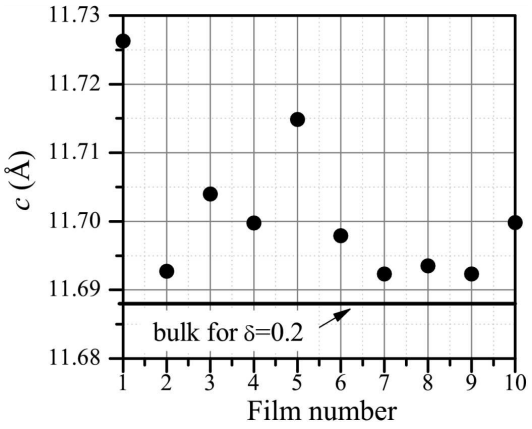

Fig. 1. Lattice constant c for set of ten $YBa_2Cu_3O_{7-\delta}$ films on CeO_2 buffered sapphire.

In all films the c-axis parameter is somewhat larger than in the bulk YBCO (shown by the continuous line for $\delta = 0.2$). We note first that the deviation of the c parameter from the bulk value is quite random, indicating that the variation is not caused by any deterioration of the deposition parameters during the growth of ten consecutive samples. The variable expansion of the c likely originates from a combination of two effects. First, the strain relaxation may take place, because the in-plane lattice constant of CeO_2, equal to 5.411 Å, induces small in-plane compressive strain in the YBCO lattice cell, which grows rotated by 45° in the CeO_2 basal plane. The second effect may be variable oxygen deficiency, which also leads to the increase of c [10]. The detailed examination of the X-ray data indicates that the (007) X-ray diffraction peak is narrow but asymmetric in all the samples which display c close to the bulk value. Such asymmetry suggests that the strain is relaxed across the thickness of the film, which is likely accompanied by the increase of the oxygen content. On the other hand, the (007) peak is wider but symmetric in the samples with the largest c-value (films 1 and 5). Thus, these films appear to be more uniformly strained and oxygen deficient throughout the film thickness.

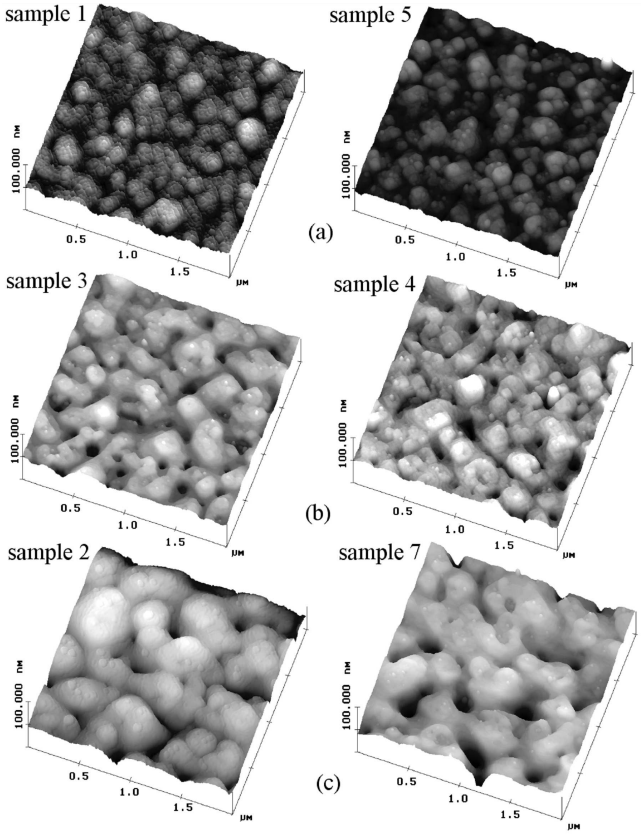

Fig. 2. AFM images of YBCO films. (a) Small (10–100 nm) grains. (b) Medium (100–200 nm) grains. (c) Large (200–500 nm) grains.

Figure 2 shows the AFM images for some (representative) films. The images suggest that the growth proceeds via island nucleation, which subsequently coalesce forming continuous films. The nucleation of island may be triggered by the presence of structural irregularities of the buffer layer which we have observed previously [5]. The irregularities in the buffer are a remanence of the grainy microstructure of as-deposited CeO_2. During recrystallization of CeO_2 the grains coalesce forming film with a small root-mean-square (RMS) roughness, of about 1.3 nm, but with a collection of shallow voids distributed across the buffer surface. Figure 2 shows furthermore

that the size of the grains in the YBCO films varies, from small (10–100 nm) in films 1 and 5, through intermediate (100–200 nm) in films 3 and 4, to large (200–500 nm) in films 2 and 7. The origin of different grain size may be related to the surface roughness of CeO_2 buffer layers, which varies slightly from sample to sample despite exactly the same recrystallization conditions. Larger surface roughness of the buffer may result in larger density of island nucleation, leading to a smaller grain size.

Interestingly, there exists a correlation between the grain size and the magnitude of the c-axis parameter shown in Fig. 1. Specifically, films 1 and 5, with the largest c, show the smallest grains. On the other hand, the films 2 and 7, with the c closest to the bulk value, but accompanied by relaxation of the c across film thickness, exhibit largest grain size. The mechanism responsible for such correlation is not exactly clear at the moment. One possibility is that the films with large grains exhibit also larger voids at the grain boundaries, which facilitates better oxygen intake during the film growth, and therefore promotes the decrease of the c parameter.

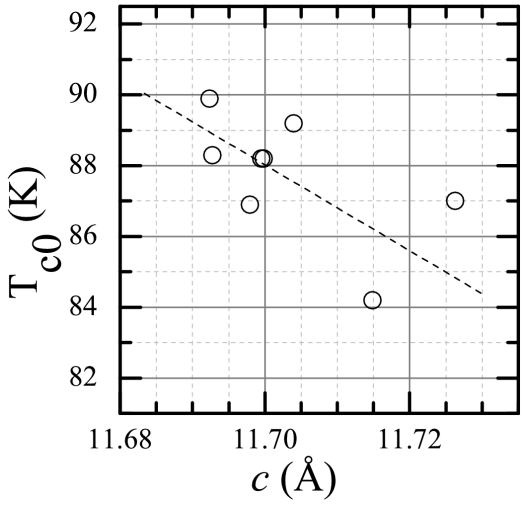

Fig. 3. The critical temperature T_{c0} of YBCO films versus lattice constant c.

We now turn attention to the superconducting properties of YBCO films. Figure 3 shows the dependence of the T_{c0} on the c-axis lattice parameter. The dashed line is drawn to indicate that, on the average, the T_{c0} decreases with increasing c. This agrees with the expectation that large c value is accompanied by oxygen deficiency. However, there is considerable scatter of the data around dashed line, suggesting that, besides oxygen deficiency, some additional factor influences the T_{c0}. This factor may be the grain boundary scattering, which should be larger when the grains are small and the density of grain boundaries is large. Unfortunately, the estimate of the grain size from AFM images cannot be correlated exactly with the transport data, because they are not measured on precisely the same film area.

Figure 4 shows the T-dependence of j_c, measured for most of the ten films deposited on CeO_2, and for one of the films grown on SAT-CAT-La substrate. We observe that $j_c(T)$ dependences may be divided into two groups, as marked in the figure. Group I contains the films, in which j_c rises quite steeply with the decreasing T. All the films which belong to this group are the ones in which c is small. The sample with the steepest increase of j_c is the film 7, with the smallest c. Group II contains the films with substantially lower j_c, and two of these films display large c value. Thus, it appears that the j_c follows similar general trend as the T_{c0}, that is, the decrease with increasing c, suggesting that the oxygen deficiency may be the primary reason for lowering of j_c. However, just as it is the case with the T_{c0}, there is no one-to-one correspondence between c and j_c. For example, the j_c in film 3 is much larger than in film 4, while c is larger in film 3. Therefore, there must be additional factor affecting the j_c, presumably related to the film microstructure.

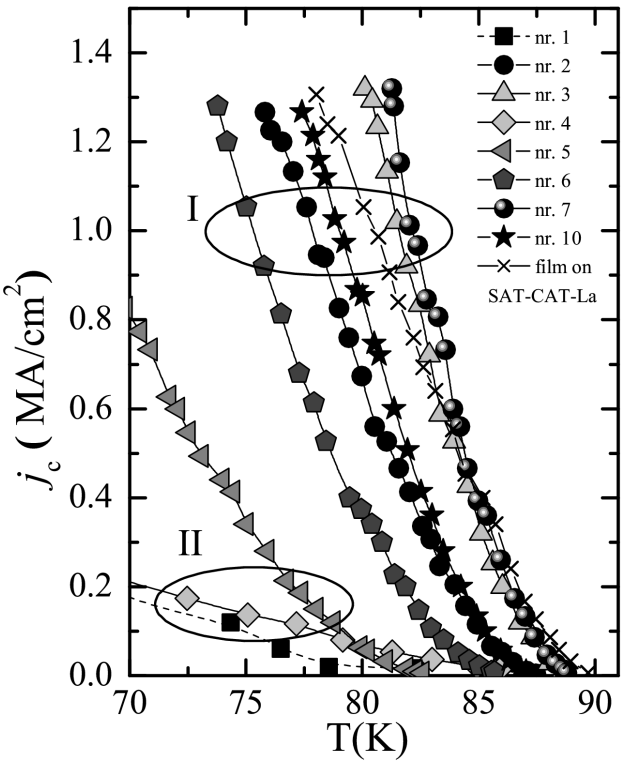

Fig. 4. The T-dependence of j_c for several YBCO films. I and II denote two groups of films with high and low j_c, respectively.

The transport measurements of j_c are restricted to high temperatures, because of the limitation on the maximum current density used in the measuring setup. To evaluate the low-T behavior of the j_c, we use magnetooptical method of the visualization of magnetic flux penetration into the film. These measurements show that the j_c increases linearly with decreasing T down to 4 K. The linear dependence of j_c on T suggests a presence of strong pinning by correlated defects, rather than the weak col-

lective pinning, which would produce exponential decay of the j_c with increasing T [11, 12].

The YBCO for application in devices should exhibit high j_c values at $T \approx 77$ K. Extrapolating the data from Fig. 4 down to $T = 77$ K we obtain j_c values in the range between 1.35 and 2.4 MA cm^{-2} for the three best films deposited on CeO_2, while the value for the film grown on SAT-CAT-La is about 1.5 MA cm^{-2}. Thus, the magnitude of j_c in the best films grown on CeO_2 exceeds the magnitude obtained for well-matched substrate. Such value of j_c is acceptable for applications of these films in the microwave devices and fault current limiters.

To discuss the possible origins of strong pinning, it is useful to examine the dependence of the j_c on the orientation of the external magnetic field H, as depicted in Fig. 5. We observe that a single sharp peak appears when the field is applied parallel to the *ab*-plane. In one of the previous studies of YBCO grown on CeO_2, in addition to the peaks near *ab* plane, the enhanced j_c has been observed near *c* axis, and attributed to the self--assembled nanodots on the CeO_2 buffer surface [13]. In the present study we do not see any evidence of such defects. Instead, the peaks near *ab* plane are commonly observed in thin films of YBCO. They indicate strong pinning by correlated disorder due to layering near *ab* plane of second-phase precipitates, stacking faults or intergrowths [12, 14]. This conclusion does not mean that the buffer-related defects do not play any role, only that they do not introduce any correlated disorder away from *ab* plane. Indeed, the correlation between the j_c and the film microstructure suggests that the buffer-related structural inhomogeneities, together with oxygen content in the films, affect the j_c.

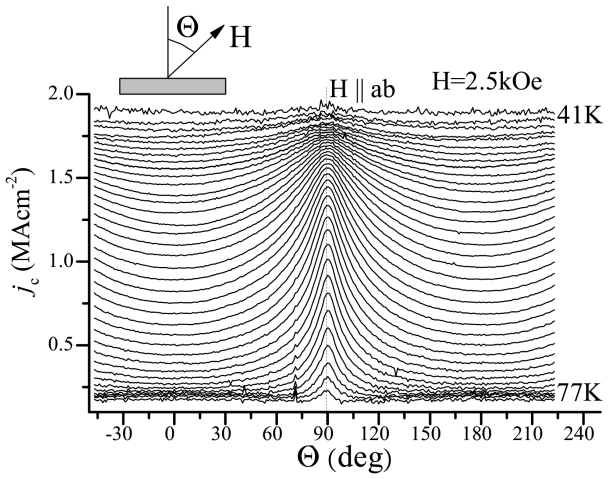

Fig. 5. The dependence of j_c on the field orientation angle Θ, measured for temperatures between 41 and 77 K, in 2 K intervals. The Θ is the angle between the field direction and perpendicular to the sample plane.

In conclusion, we have deposited a set of YBCO films on CeO_2-buffered sapphire to examine the growth process and access the suitability of such films for applications in devices. We observe that there is a noticeable correlation between the structural and microstructural properties of the films and the superconducting parameters, the T_{c0}, and the j_c. The best films, with highest value of j_c, suitable for applications, are the films in which the strain introduced by the buffer layer is relaxed, and the growth proceeds by nucleation of large grains.

Acknowledgments

This work was supported by the European Union within the European Regional Development Fund, through the Innovative Economy grant POIG.01.01.02-00-108/09, and by the French-Polish Bilateral Program PICS 2012.

References

[1] R.W. Simon, R.B. Hammond, S.J. Berkowitz, B.A. Willemsen, *Proc. IEEE* **92**, 1585 (2004).

[2] M. Lorenz, H. Hochmuth, D. Natusch, M. Kusunoki, V.L. Svetchnikov, V. Riede, I. Stanca, G. Kästner, D. Hesse, *IEEE Trans. Appl. Supercond.* **11**, 3209 (2001).

[3] K. Ohki, K. Develos-Bagarinao, H. Yamasaki, Y. Nakagawa, *J. Phys. Conf. Series* **97**, 012142 (2008).

[4] J.C. Nie, H. Yamasaki, Y. Nakagawa, K. Develos-Bagarinao, M. Murugesan, H. Obara, Y. Mawatari, *J. Phys. Conf. Series* **43**, 353 (2006).

[5] I. Abal'osheva, I. Zaytseva, M. Aleszkiewicz, Y. Syryanyy, P. Gierłowski, O. Abal'oshev, V. Bezusyy, M.Z. Cieplak, *Acta Phys. Pol. A* **121**, 805 (2012).

[6] I.S. Abal'osheva, M.Z. Cieplak, Z. Adamus, M. Berkowski, V. Domukhovski, M. Aleszkiewicz, *Acta Phys. Pol. A* **109**, 549 (2006).

[7] Ch. Joos, A. Forkl, R. Warthmann, H. Kronmuller, *Physica C* **299**, 215 (1998).

[8] J. Gilchrist, M. Konczykowski, *Physica C* **212**, 43 (1993).

[9] C.J. van der Beek, M. Konczykowski, V.M. Vinokur, G.W. Crabtree, T.W. Li, P.H. Kes, *Phys. Rev. B* **51**, 15492 (1995).

[10] P.K. Gallagher, H.M. O'Bryan, S.A. Sunshine, D.W. Murphy, *Mater. Res. Bull.* **22**, 995 (1987).

[11] C.J. van der Beek, M. Konczykowski, V.M. Vinokur, T.W. Li, P.H. Kes, G.W. Crabtree, *Phys. Rev. Lett.* **74**, 1214 (1995).

[12] O. Polat, J.W. Sinclair, Y.L. Zuev, J.R. Thompson, D.K. Christen, S.W. Cook, D. Kumar, Y. Chen, V. Selvamanickam, *Phys. Rev. B* **84**, 024519 (2011).

[13] J.C. Nie, H. Yamasaki, H. Yamada, Y. Nakagawa, K. Develos-Bagarinao, Y. Mawatari, *Supercond. Sci. Technol.* **17**, 845 (2004).

[14] C.J. van der Beek, M. Konczykowski, A. Abal'oshev, I. Abal'osheva, P. Gierłowski, S.J. Lewandowski, M.V. Indenbom, S. Barbanera, *Phys. Rev. B* **66**, 024523 (2002).